Acta Geophysica (2019) 67:59–75
https://doi.org/10.1007/s11600-018-0210-6

RESEARCH ARTICLE - SOLID EARTH SCIENCES

Testing the performance of earthquake early warning system in northern India

Himanshu Mittal[1,2] · Yih-Min Wu[1,3] · Mukat Lal Sharma[4] · Benjamin Ming Yang[1] · Sushil Gupta[5]

Received: 14 January 2018 / Accepted: 6 October 2018 / Published online: 11 October 2018

Abstract
The main goal of present study is to test the functionality of an earthquake early warning (EEW) system (a life-saving tool), in India using synthesized data and recorded earthquake data from Taiwan. In recent time, India set up an EEW system in the central seismic gap along the Himalayan Belt, consisting of about 100 low-cost P-Alert instruments. The area, where these instruments are installed, is highly sensitive to the seismic risk with the potential of strong, major and great earthquakes. In the absence of recorded data from the Himalayas required for analysis of such system, we take advantage of recorded waveforms from Taiwan, to test the EEW system. We selected Taiwanese stations in good accordance with the Indian sensor network, to have a best fit in terms of inter station spacing. Finally, the recorded waveforms are passed through Earthworm software using tankplayer module. The system performs very well in terms of earthquake detection, P-wave picking, earthquake magnitude and location (using previously estimated regressions). P_d algorithm has been tested where the peak amplitude of vertical displacement is used for estimating magnitudes using previously regressed empirical relationship data. For the earthquakes located between Main Boundary Thrust and Main Central Thrust along with a matching instrumentation window, a good estimate of location, as well as magnitude is observed. The approach based on P_d for estimating magnitude works perfectly as compared to τ_c approach, which is more sensitive to signal-to-noise ratio. To make it more region specific, we generated synthetic seismograms from the epicenters of historical Chamoli (1999) and Uttarkashi (1991) earthquakes at EEW stations in India and checked the functionality of EEW. While placing these earthquakes within the instrumentation window, a good approximation of earthquake location and magnitude is obtained by passing these generated waveforms. The parameters used to judge the performance of EEW system included the time taken by the system in issuing warning after the confirmation of the occurrence of damaging earthquake and the lead time (time interval between the issuing of warning and arrival of damaging earthquake ground motion at a particular location). High lead times have been obtained for the plainer regions including thickly populated regions of Gangetic plains, such as Delhi National Capital Region according to the distance from the epicenter, which are the main target of EEW system.

Keywords Central seismic gap (CSG) · Earthquake early warning (EEW) · Earthworm software · NCR · Vertical displacement P_d

Introduction

Earthquakes are one of the most disastrous natural hazards, and our inability to predict its location and magnitude and its occurrence in future makes it potentially catastrophic. Since the earthquakes are unpredictable, a new approach called earthquake early warning (EEW) has been developed in the last couple of decades (Wu et al. 2016). This new approach is based on the number of instruments recording data near epicenter, communication technology (mode of transmission of data from field instruments to central processing server) and processing speed at the central seismic station.

✉ Himanshu Mittal
himanshumitt10@gmail.com

1 Department of Geosciences, National Taiwan University, Taipei 10617, Taiwan

2 Present Address: Department of Earth Sciences, National Cheng Kung University, Tainan, Taiwan

3 Institute of Earth Sciences, Academia Sinica, Taipei, Taiwan

4 Department of Earthquake Engineering, Indian Institute of Technology, Roorkee, India

5 Risk Modeling and Insurance, RMSI, Noida, India

The basic concept of EEW relies on identifying the early portion of earthquakes in movement and issuing a warning to surrounding population areas, well ahead before the occurrence of damaging ground shaking (Wu and Kanamori 2005b). There are two types of EEW algorithms, namely on-site and regional, and each of them uses data from the nearby stations to accurately estimate the shaking intensity of an event from early portion of the wave. On-site or local warning approach takes advantage of the fast propagating P waves, which moves at much higher speed than the S-waves carrying more energy. As soon as the first P wave is observed, it is analyzed to determine the expected intensity of the earthquake and if found to be potentially dangerous, a warning is issued. On the other hand, regional or network-based early warning system uses data from a seismic network next to the epicenter area to rapidly detect and locate an earthquake, determine its magnitude and predict the ground motion at distant places.

During last three decades, there has been tremendous growth concerning installation and functioning of EEW in different part of the world. EEW is working successfully in countries like Japan (Nakamura 1988; Hoshiba et al. 2008; Kamigaichi et al. 2009; Brown et al. 2011), Taiwan (Wu and Zhao 2006; Hsiao et al. 2009; Wu et al. 2018), Mexico (Espinosa-Aranda et al. 2009), Romania (Wenzel et al. 1999; Böse et al. 2007; Ionescu et al. 2007) and around Anatolia (Erdik et al. 2003; Alcik et al. 2009; Legendre et al. 2017). EEW system of Mexico utilizes the peak ground motion (PGM), to issue a 60 s or more warning to the public in Mexico City (around 300 km away) from an earthquake occurring near the Guerrero Gap subduction zone (Espinosa-Aranda et al. 1995). This system provided Mexico City an early warning time of about a minute in the very recent two major magnitude earthquakes of September 8, 2017 (M 8.1) and September 19, 2017 (M 7.1), which focused the attention of the entire community on the dangers of major and great earthquakes, thanks to Mexico's effective EEW system, which has reduced the significant number of causalities.

Depending upon the location of occurrence of the earthquake, the warning time in Japan may range from a few seconds to 40 s. Taiwan provides warning alert to authorities and in recent time to the public (Wu 2015; Chen et al. 2015; Wu et al. 2016). In some countries, EEW is under development or testing stage like California (Allen and Kanamori 2003; Allen et al. 2009; Böse et al. 2009; Brown et al. 2011), Southwest Iberia (Pazos et al. 2015; Petit et al. 2016), Southern Italy (Zollo et al. 2006, 2009), Switzerland (Cua and Heaton 2007) and India (Kumar et al. 2014). A lot of studies have been carried out using regional EEW approach (Allen and Kanamori 2003; Kanamori 2005; Wu and Kanamori 2005a, b, 2008; Wu et al. 2006, 2007; Yamada and Heaton 2008; Satriano et al. 2011; Carranza et al. 2013).

The performance of EEW system is judged according to the time taken by the system in issuing warning after the confirmation of the occurrence of damaging earthquake and the lead time (time interval between the issuing of warning and arrival of damaging earthquake ground motion at a particular location). This lead time varies from a couple of seconds to tens of second at different locations according to the distance from the epicenter. Areas in India covered under severe seismic hazard are the Himalayan Belt in the north from Kashmir to Manipur, Gujarat in the west and Andaman & Nicobar Islands in the southeast. The great Himalaya is formed because of continuing collision between Indian and Eurasian plates (Legendre et al. 2015a, b). Not so frequent, but earthquakes of varying magnitudes keep on occurring along the Himalayan Belt. Some large magnitude earthquakes are documented along the Himalayan Belt in last 200 years (Fig. 1). Whereas the western part experienced earthquakes in 2005, 1905, the eastern part experienced 1833, 1934, 1950 and 2015 earthquakes, for almost last 65 years, no big earthquake occurred along this belt, though it has the potential to generate some bigger one. Such segments, which are considered the future locale of major and great earthquakes, are referred as seismic gaps. One such kind of seismic gap is the central seismic gap (CSG), which lies between the eastern edge of the 1905 rupture zone and the western edge of the 1934 earthquake (Fig. 1); where no major earthquake occurred for last more than 100 years (Bilham 1995). Khattri (1999) predicted the probability of happening of a great earthquake in CSG to be 0.59 in the next 100 years. Various seismic hazard exercises have already given high probabilities of occurrence of damaging earthquakes in northern Indian region (Sharma and Lindolhm 2012; Sharma 2003). Some lower magnitude earthquakes occurred in CSG in 1803 and 1833 (Seeber and Armbruster 1981), but were not gap filling as the magnitude for both of these events was less than 8 (Khattri 1999; Bilham 1995). However, in recent time, an earthquake with M_w 7.9 occurred in the central Nepal region, but this earthquake also occurred out of CSG. A major/great earthquake in the CSG is likely to cause colossal loss of life and property, as the areas in the Himalayan foothills and plains in northern India are highly populated with the majority of the buildings as non-engineered (Wyss et al. 2017). This accentuates the need for the realistic assessment of ground motion from future earthquakes in the CSG. Taking into consideration the lead time, northern India can utilize EEW in a practical way, where damaging earthquake sources lie in the Himalayan region, while densely populated areas, as well as industrial hubs, are located in the Himalayan foothills and plains far away from source zone. Even few seconds warning is useful as it will be sufficient for shutting down of nuclear power plants (Gupta 2000), gas pipelines, slowing down of the high-speed trains and metro rails and most importantly

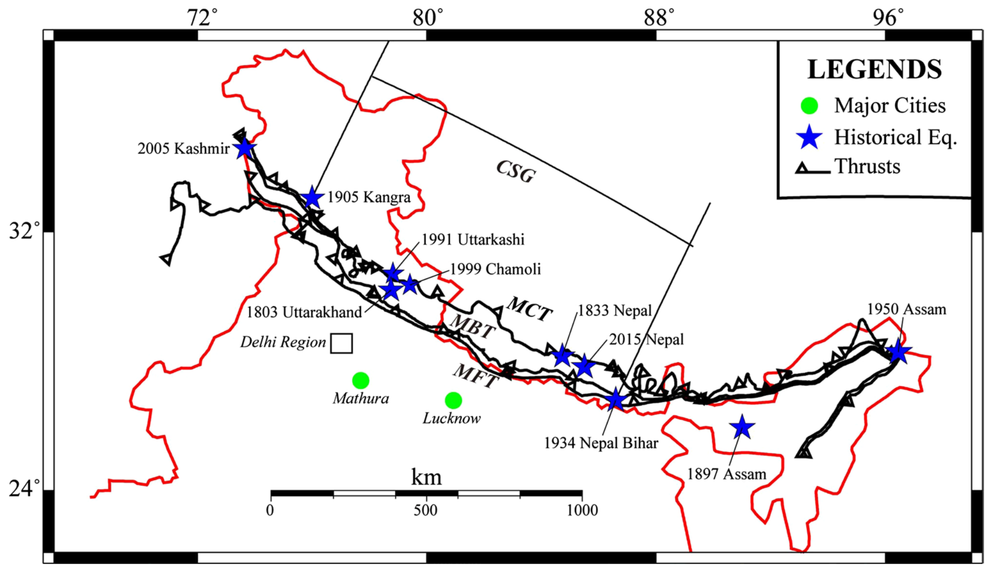

Fig. 1 Location map of Indian Himalayas. Main prominent thrusts, namely Main Central Thrust (MCT), Main Boundary Thrust (MBT) and Main Himalayan Thrusts (MHT) are plotted in the figure. Greater magnitude historical earthquakes occurred along Himalayan arc are plotted. Central seismic gap (CSG) marked between the 1905 Kangra earthquake and the 1934 Nepal Bihar earthquake is the future locale of greater magnitude earthquake (Khattri 1999)

saving precious lives as people can move to safer or nearly safer place (Bhardwaj et al. 2016). A further larger early warning period can be useful for coming out of unsafe and high-rise buildings. For earthquake disaster mitigation, a successful EEW system can be the keystone. In present work, the performance of EEW in northwest Himalaya is discussed using earthquake recorded ground motion data from Taiwan and synthetic waveforms.

Instrumentation

Department of Earthquake Engineering (DEQ), Indian Institute of Technology, Roorkee (IITR), in support of Ministry of Earth Sciences (MoES), India, initiated an EEW system along the Himalayan Belt in India. Under this project, about 100 instruments are installed in a specified window in CSG (Fig. 2). In general, the distance between the stations is kept to be 15–20 km. It is in accordance with ElarmS guidelines (Allen et al. 2009), which states that for an ideal EEW in operation, the general spacing between the instruments should be less than 20 km. However, due to the presence of various faults along the Himalayan Belt, this spacing should be further reduced for an effective EEW. As the Himalayan Belt is very large and Indian government plan to install EEW system along the whole Himalayan Belt in future, traditional force-balanced accelerometers (FBAs) may not be an efficient choice because of financial implications. Instead, a low-cost microelectromechanical system (MEMS)-based seismic network will be a better choice for EEW in India.

The P-Alert is a P-wave detecting device, devised by National Taiwan University (NTU) research team in collaboration with some private organization. It is a tiny and low-cost sensor with MEMS technology embedded inside. The cost of P-Alert is much lesser than the usual FBAs. The system is designed to record three-component data stream along x, y and z directions. The signal resolution is 16 bits with ±2 g dynamic range. The real-time data from P-Alert are transmitted after every second through the internet. In addition, this instrument has P_d technology embedded inside to work as an on-site warning system. Since P-Alert works in continuous mode, the data in each of the instruments in the field are processed for P-wave detection and is continuously double integrated for estimating the peak amplitude of displacement, P_d (Wu and Kanamori 2005b). Once the captured signal exceeds predefined thresholds (P_d larger than 0.35 cm based on previous regressions) or PGA larger than 80 gals, the P-Alert device begins sending an alert with a warning sound for on-site EEW purposes (Kanamori 2005; Wu and Kanamori 2005a, b; Wu et al. 2011, 2013).

In addition, P-Alert can be used as a regional EEW system (Kanamori 2005; Wu and Kanamori 2005a) through the Internet. The P-Alert EEW system results in Taiwan have been reported several times (Wu et al. 2013), but for Indian region no such types of effective alerts are available currently. Figure 2 shows the EEW P-Alert network in India along with some of the main faults responsible for seismicity in the Himalayas. The data stream from each field instrument is transferred continuously to the central processing system (NTU in Taiwan and IITR in India). The data at the central seismic station are processed and stored within the Earthworm system (an open source software) developed by the US Geological Survey (Johnson et al. 1995; Chen et al. 2015).

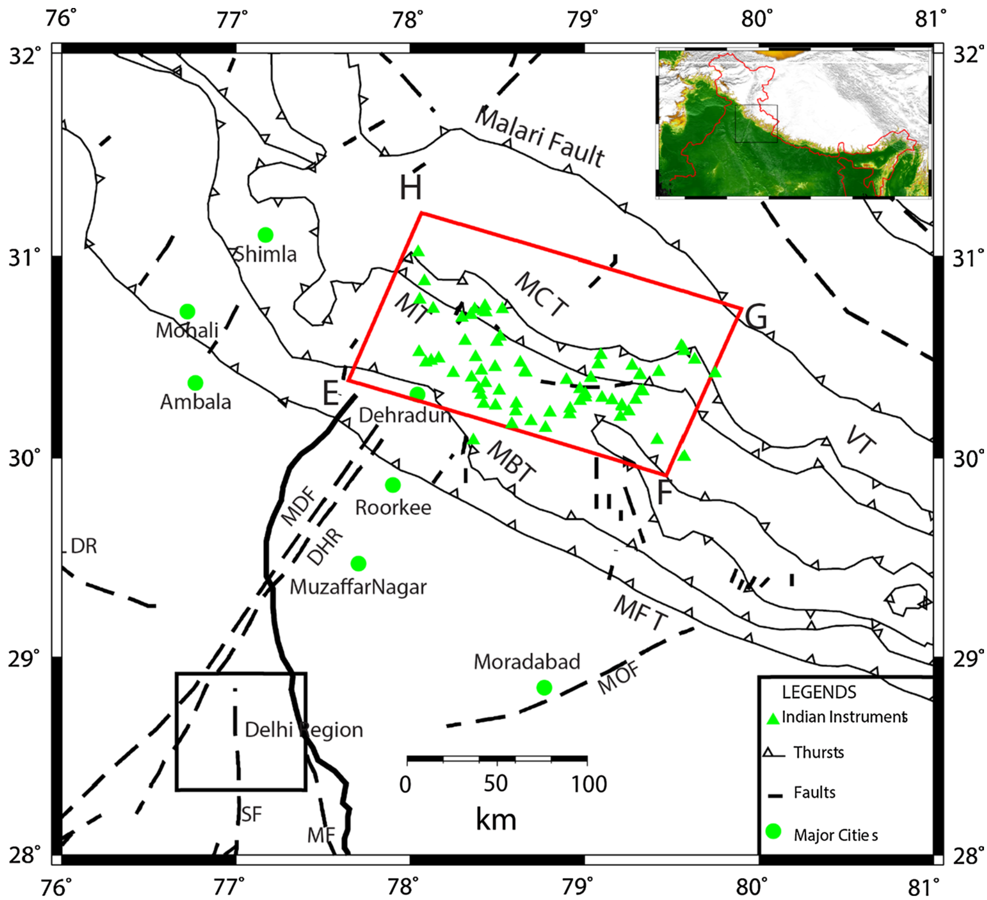

Fig. 2 Map showing the location of earthquake early warning systems (EEWS) deployed by Indian Institute of Technology, Roorkee. Main thrusts like MCT, MBT, MFT and other faults are also plotted. This EEWS may be beneficial regionally for cities lying in plain especially Delhi National Capital Region (NCR), about 250–300 km away from Himalayan range

Coordinates mapping

The geodetic coordinates (latitude and longitude) of stations from Taiwan window are mapped into Indian window for checking the functionality of EEW system in Indian region. Before making use of the data recorded from Taiwan arrays, their mapping has been carried out. As the two regions are seismically very active and being in compressional environment, the earthquake occurrence for the damaging earthquakes in these regions is thrust type. Moreover, the strong motion being recorded in near field, the effect of difference in the medium characteristic is minimized. The interstation distances of the two arrays are similar, and therefore, the intrinsic and/or the geometrical attenuations will have either no effect on the comparisons of the amplitudes of the recorded data or the effect will be minimal to validate the coordinate mapping approach. For this, the geodetic coordinates of Taiwan stations are derived into their distances and angles with reference to the original reference point (Taiwan window). Based on the idea of two straightforward rules: (1) the ratio of the original distance to the new distance is equal to the ratio of the length of the original reference line to the new reference line, and (2) the angle between line SR (station-reference point) and the reference line remains constant, and we obtain the new distances and angles in reference to the new reference point of the stations (Indian window). Finally, the new distances and angles are used to derive the converted geodetic coordinates in Indian window.

As shown in Fig. 3, the reference point and reference line in the original window are fixed. A station is placed within the original window, whose geodetic coordinates are known. Using the Inverse Vincenty's formula (Vincenty 1975), the distance r between the station and reference point as well as the angle θ between line SR (station-original reference point) and the original reference line is derived. In next step, we obtain the enlarge factor given by:

$$\text{Enlarge factor} = \frac{\text{Length of new ref. line}}{\text{Length of original ref. line}}$$

According to rule 1, the distance r is multiplied by the enlarge factor to obtain the new distance r between the station and the reference point in the new window. By rule 2, we know that the new angle θ between line SR (station-new reference point) and the new reference line

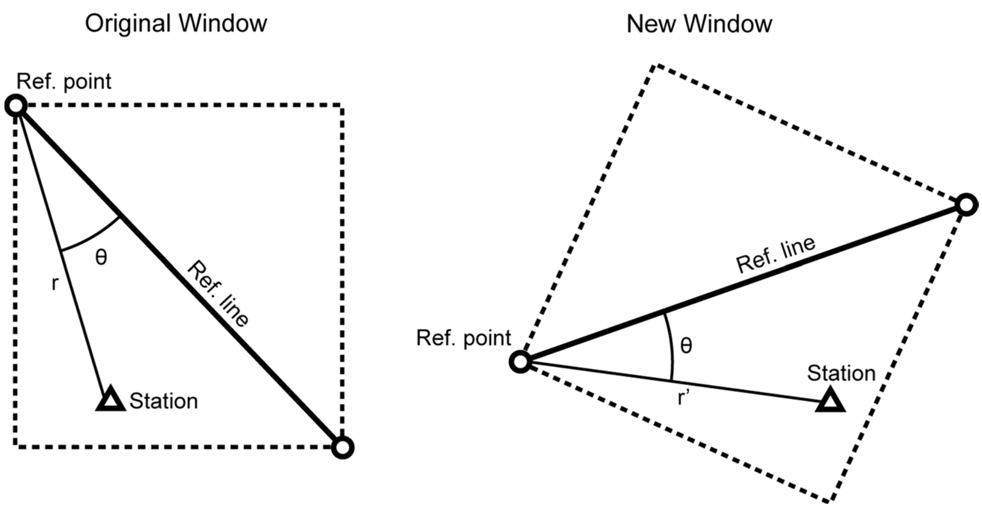

Fig. 3 The process of transforming coordinates from one place to another

is same as the original one. ABCD is the window chosen from Taiwan, where A is reference point, and AB is the reference line. In the same way, EFGH is the chosen window from India, where E is the reference point and EF is reference line (Fig. 4). In Taiwan, P-Alerts are installed densely along whole Taiwan belt at every 5–10 km, while India started EEW by placing around 100 instruments at a distance of about 20 km. A specific window is chosen from Taiwan corresponding to the Indian window. In India, these instruments are installed in 150 km × 60 km window; however, some of the instruments still lie outside the window. To overcome this problem, we choose a bigger window 180 km × 100 km from India. However, having similar dimension window from Taiwan is difficult, but we still manage to select one. As shown in Fig. 4, coordinates transformation is made according to the bigger windows in India as well as Taiwan.

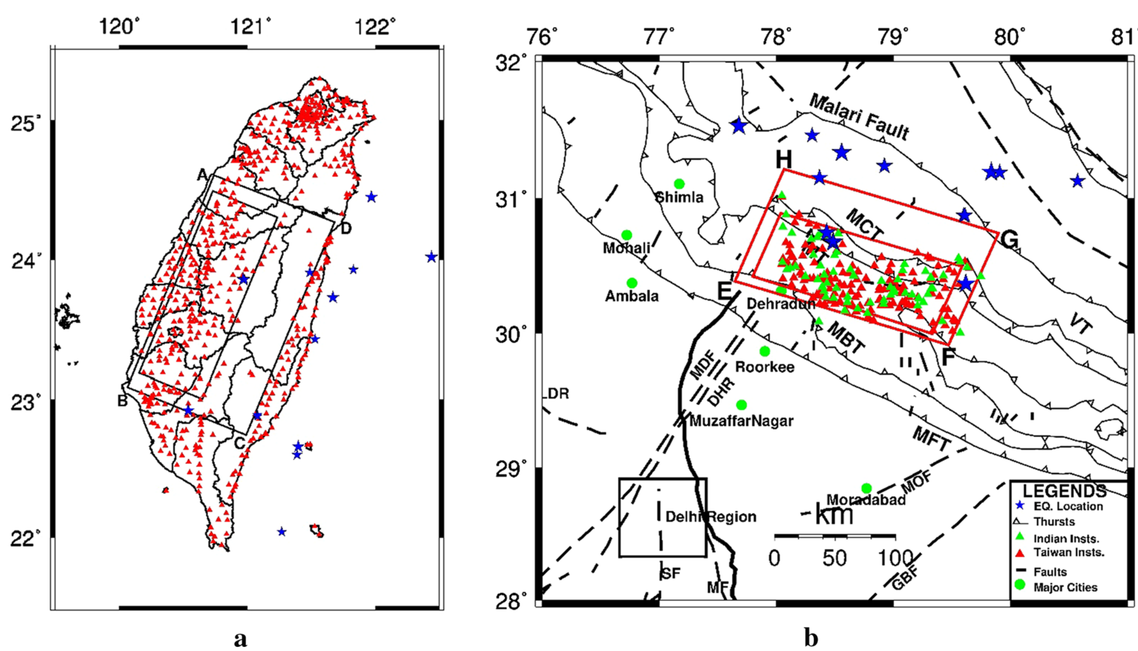

Fig. 4 Transformation of instruments location from Taiwan to India using approach is depicted in Fig. 3. A rectangle window of same size is chosen from India as well as Taiwan. A number of earthquakes having magnitude ≥ 5.5 are chosen from Taiwan. After transforming Taiwan instruments in Indian coordinates, only instruments that fall close to actual Indian EEW are chosen for processing

Processing

The pre-recorded data of various channels from each earthquake are concatenated into a single file, called Tank file. This file can be played in Earthworm software in order of the timestamp of each record line. By this method, we could pass the recorded data to our algorithm in a similar manner, as it would have streamed during real-time event. The algorithm is then tested, and the parameter values can be optimized. Earthworm module Pick_EEW automatically detects the P-wave arrival, and the peak values of displacement (P_d), velocity (P_v) and acceleration (P_a) are estimated from 3 s time window after the P-wave arrival. Another parameter characteristic period (τ_c) is also estimated from 3 s window after P arrival. τ_c estimation uses the frequency content of P wave, while other parameters P_d, P_v and P_a adopt the amplitude content of the initial waveforms. The peak value of P_a is picked directly from seismograms, while these seismograms are integrated and double integrated to get the values of P_a and P_d, respectively. A high-pass 0.075 Hz recursive Butterworth filter is applied to remove low-frequency drift during the integration process. The τ_c approach for calculating magnitude was introduced by Wu and Kanamori (2005b) after modifying Nakamura (1988). This approach looks appealing; however, finding magnitude using this approach misleads sometimes because it is more sensitive to signal-to-noise ratio (Shieh et al. 2011). The information from Pick_EEW is transferred to another shared memory Pick_Ring, which in turn provides information to TCPD module for calculation of earthquake source parameters. On detection of earthquake, the TCPD module updates information about the event and sends it to another module called Hypo_Ring, where they are stored temporarily. The earthquake messages are filtered using specific criteria in DCSN module based on previous regression by Wu and Kanamori (2005b, 2008). Once predefined thresholds are exceeded and the location is known, the reports are generated and a warning is issued. This algorithm for estimating various EEW parameters is shown in Fig. 5.

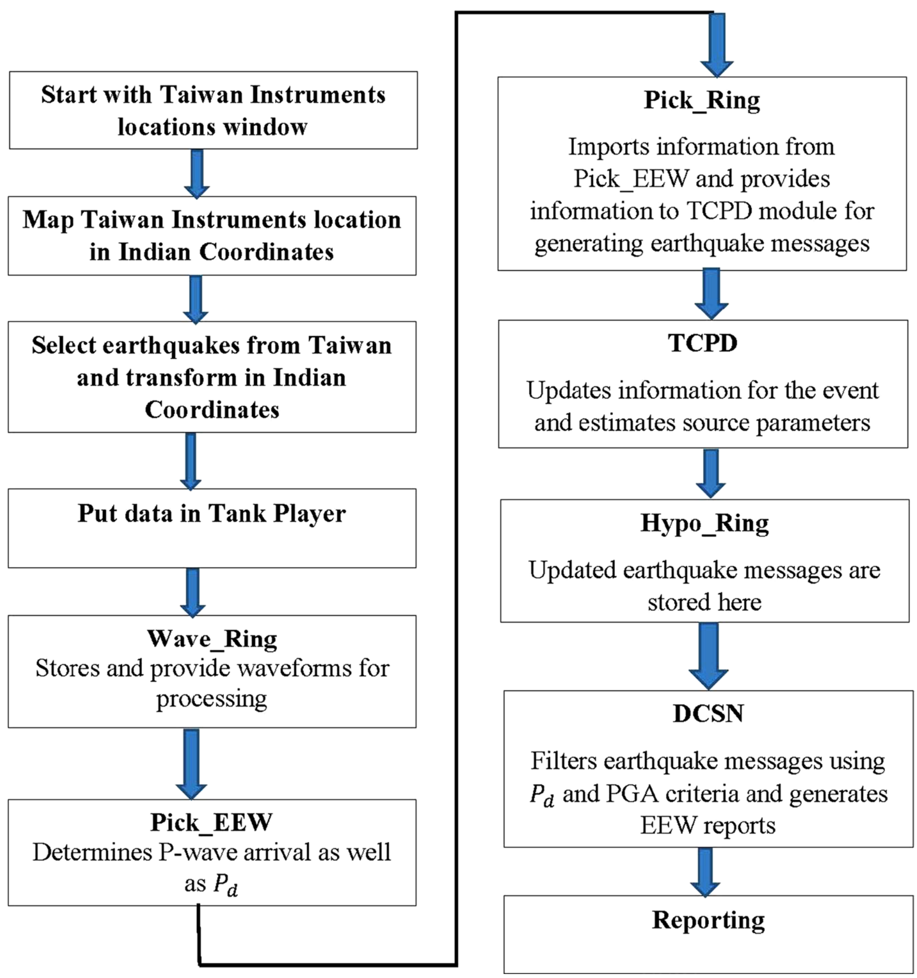

Fig. 5 Various steps involved in estimating various earthquake early parameters and generation of reports

Table 1 The list of earthquakes selected from Taiwan as well as transformed in India

Earthquake	Magnitude	Taiwan coordinates		Indian coordinates		Depth
		Latitude	Longitude	Latitude	Longitude	
20130327	6.2	23.90	121.05	30.75	78.43	19.4
20130602	5.0	22.04	121.27	31.13	80.57	31.5
20130602	6.5	23.86	120.97	30.68	78.48	14.5
20131031	6.4	24.45	121.97	31.53	77.68	10.0
20140115	5.0	23.86	120.98	30.69	78.48	15.0
20140115	5.1	22.89	121.08	30.87	79.60	8.3
20140115	5.1	22.88	121.08	30.87	79.61	8.4
20150214	6.3	22.66	121.40	31.19	79.84	27.8
20150323	6.2	23.73	121.67	31.34	78.56	38.4
20150420	6.4	24.02	122.44	32.01	78.12	30.6
20150901	5.5	23.91	121.49	31.15	78.37	17.1
20151105	5.0	23.93	121.83	31.46	78.30	47.9
20151203	5.3	22.60	121.39	31.19	79.91	25.1
20160111	5.3	23.43	121.53	31.24	78.92	28.6
20160206	6.6	22.92	120.54	30.37	79.62	16.7

Results and discussion

The area, where EEW instruments are installed in India, is highly sensitive to seismic risk with possible occurrence of the higher magnitude earthquake. Since the sensors that we have selected for simulation are P-Alert and currently no recorded data are available for higher magnitude events in India, we use recorded data of Taiwan. A number of different magnitude earthquakes are selected from Taiwan (Fig. 4a and Table 1) and are transferred to Indian coordinates (Fig. 4b and Table 1) with the same procedure as that of instruments. Since it is difficult to find all higher magnitude earthquakes close to instruments grid, we selected some earthquakes onshore while other offshore from Taiwan. Finally, the recorded waveforms are passed through the Earthworm software (Johnson et al. 1995; Chen et al. 2015) using tankplayer module and various EEW parameters are estimated.

Original TCPD approach inherited from Taiwan uses the Taiwan velocity model to calculate various parameters. This velocity model gives reasonable results when using in Taiwan with Taiwan instruments. However, after transforming instruments as well as earthquake locations from Taiwan to India, we performed experiments using Taiwan velocity model, Indian velocity model (Kumar et al. 2009) as well as Global velocity model (Kennett and Engdahl 1991) to check the applicability of EEW in India using Taiwan instruments.

Before checking these earthquakes in Indian coordinate system, we checked these earthquakes in Taiwan with original Taiwan instruments. The system responded very well, and reports were generated. Since the ABCD rectangle in Taiwan contains almost 250 instruments (Fig. 4a), the system responded very well. Though the magnitude of all earthquakes using P_d approach was close to actual one, location of some of the earthquakes (offshore) was not precise.

We tried to check the functionality of EEW approach in India initially with all these 250 instruments corresponding to EFGH rectangle (Fig. 4b). Later on, the number of instruments was reduced from 250 to as that of the actual number of instruments in India. Based upon the performance of EEW approach in Taiwan and India, finally, six earthquakes having magnitude around 6 (capable of causing damages in the plainer regions) are tested for regional EEW purpose. The system performs very well in terms of earthquake detection, P-wave picking, earthquake magnitude and location (using previously estimated regressions). The performance of system is reported in terms of EEW warning.

27/3/2013 earthquake

Global model

Various reports are generated. The first report occurs 7.3 s after the occurrence of the event. By this time, 10 instruments have been triggered. The second report comes after 8.1 s, and 11 instruments have triggered. The third report is generated after 11.0 s with 14 instruments. The fourth report comes after 14.8 s with 15 instruments. In same way, the fifth report arrives after 15.0 s with 16 instruments.

Indian model

Total 9 reports are generated. The first report comes in 5.4 s with triggering of 8 instruments. Several other reports come after 8.3 s (10 instruments), 10.5 s (12 instruments), 11.1 s (14 instruments), 11.2 s (16 instruments) and 11.3 s (18 instruments). Ninth report is generated using data from 25 instruments.

Taiwan model

Ten reports have been generated after 5.5 s (8 instruments), 8.9 s (11 instruments), 10.0 s (12 instruments), 11.1 s (13 instruments), 11.3 s (16 instruments) and so on. The tenth report comes 15.4 s later with triggering of 24 instruments.

When first report is generated using all the three models, almost 8 instruments have triggered. Using P_d approach, the magnitude is estimated to 6.1 after 6–8 s. Figure 6 shows that all tested models, probably due to the limited instruments triggered, do not accurately retrieve the location as well as depth. During the second report, somewhat less error is observed in the location with M_{P_d} 6.5 as around 10 instruments have triggered. By the time, the third report comes using all three models; a precise location is obtained. The

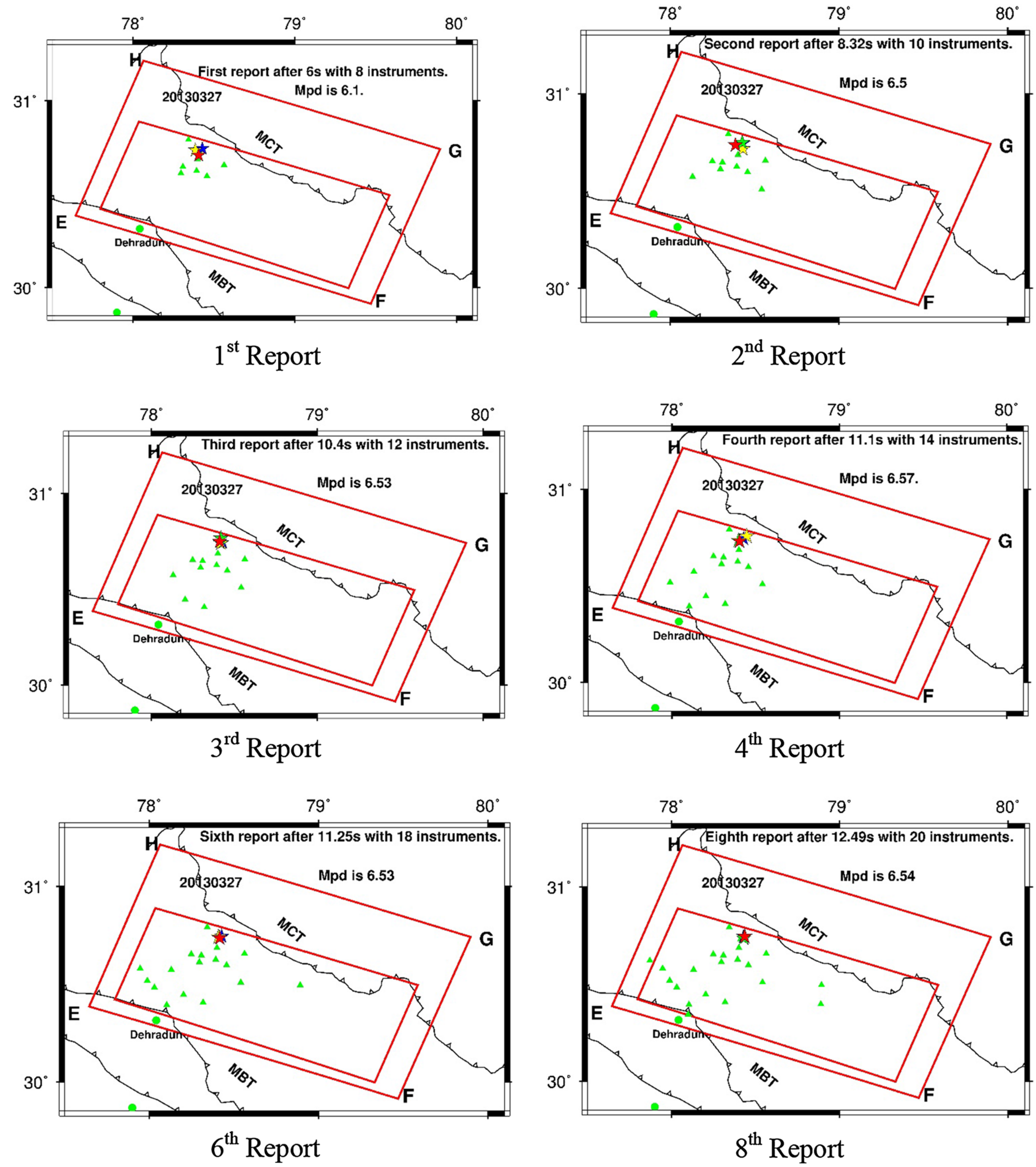

Fig. 6 Various reports generated after different time during 27/3/2013 earthquake. Blue star depicts the transformed earthquake location in Indian coordinate systems. Yellow star, green star and red star gives the location estimated in EEW system using global velocity model, Taiwan velocity model and Indian velocity model, respectively

Table 2 Comparison of location and magnitude using three different models, i.e., global velocity model, Taiwan velocity model and Indian velocity model

Earthquake	Magnitude	Location	Depth	Global				Taiwan				India			
				Coordinates	Depth	Reporting time	Magnitude	Coordinates	Depth	Reporting time	Magnitude	Coordinates	Depth	Reporting time	Magnitude
27/3/2013	M_L 6.2 M_w 6.0	30.746 78.429	19.4	30.743 78.420	14.4	10.98(3)	Mpv = 6.2 Mpd = 6.6	30.738 78.422	12.97	11.09(3)	Mpv = 6.2 Mpd = 6.6	30.733 78.404	12.98	11.11(4)	Mpv = 6.1 Mpd = 6.5
02/06/2013	M_L 6.5 M_w 6.2	30.676 78.484	14.5	30.732 78.494	11.23	8.99(5)	Mpv = 6.8 Mpd = 6.8	30.696 78.455	7.64	9.05(5)	Mpv = 6.6 Mpd = 6.7	30.698 78.458	6.58	9.34(4)	Mpv = 6.7 Mpd = 6.7
31/10/2013	M_L 6.4 M_w 6.3	31.532 77.680	10.0	30.939 78.738	6.31	16.22(4)	Mpv = 6.2 Mpd = 6.5	30.901 78.744	1.72	15.17(6)	Mpv = 6.2 Mpd = 6.3	30.925 78.758	2.26	16.42(4)	Mpv = 6.1 Mpd = 6.3
14/2/2015	M_L 6.3 M_w 6.2	31.193 79.836	27.8	30.562 78.343	7.85	14.59(2)	Mpv = 7.7 Mpd = 5.2	30.553 78.328	0.87	15.3(2)	Mpv = 5.2 Mpd = 7.7	30.733 78.404	9.12	14.17(2)	Mpv = 5.2 Mpd = 7.7
23/3/2015	M_L 6.2 M_w 6.0	31.336 78.557	38.4	31.011 78.509	12.81	16.37(3)	Mpv = 6.3 Mpd = 6.4	30.837 78.448	0.27	16.95(3)	Mpv = 6.2 Mpd = 6.2	30.698 78.458	35.48	17.72(2)	Mpv = 6.7 Mpd = 6.4
06/02/2016	M_L 6.6 M_w 6.4	30.368 79.618	16.7	30.345 79.537	8.35	16.24(3)	Mpv = 6.6 Mpd = 6.7	30.352 79.538	1.02	17.98(4)	Mpv = 7.0 Mpd = 6.9	30.925 78.758	4.17	16.63(3)	Mpv = 6.5 Mpd = 6.6

estimated magnitude (M_{P_d} = 6.5), as well as depth, is close to actual one. The actual magnitude of the earthquake is 6.2, while using different models it comes around 6.5–6.6 (Table 2). As the location of earthquake source lies within instrumentation window, the inclusion of data close to the source having large near-field terms may lead to high P_d and P_v values and consequently higher magnitude (Yamada and Mori 2009). Out of three models, Indian velocity model seems to respond in an efficient way as it provides magnitude, location and depth close to actual one compared with the other two models (Fig. 6).

2/6/2013 earthquake

This earthquake is located within the instrumentation window. As soon as the earthquake is triggered, many instruments are triggered and a large number of reports are generated. These reports are generated because system chooses records from the different instruments and generate a report. During this earthquake, the system responds very well and starts generating reports only 7.0 s after the occurrence of the earthquake with the triggering of minimum 8 instruments. By the time, 4th report is generated with elapse of 9.5 s; a precise location, as well as magnitude, is found (Fig. 7). The total number of triggered instruments is 14. Around 15–20 reports are generated using each model. During this earthquake, all the three models provide precise results. The earthquake magnitude is 6.5, while it is reported between M_{P_d} = 6.7–6.9 using three different models. Using all three models, the difference in depth is observed. The closest depth estimate is found using global velocity model. This earthquake was also within instrumentation window and so may be overestimated due to near-field term.

31/10/2013 earthquake

This earthquake is located toward northwest far away from instrumentation window. The system responds to this earthquake, but the location is not precise. Firstly, the system takes much time around 11 s to generate the first report with triggering of 10 instruments. Even after detection of the earthquake with 10 instruments, the earthquake is located toward the north of instrumentation window. By the time the fourth report is generated (which we consider being reliable) with triggering of 16 instruments, 16.0 s has elapsed and still location as well as depth is very far away from the actual one (Fig. 7). The estimated magnitude using all three models is found reasonable (M_{P_d} = 6.3–6.5). In Taiwan also, this earthquake is located offshore and was not located precisely by EEW system of Taiwan. The simple reason for this may be the recording station coverage as no station is available close to earthquake location.

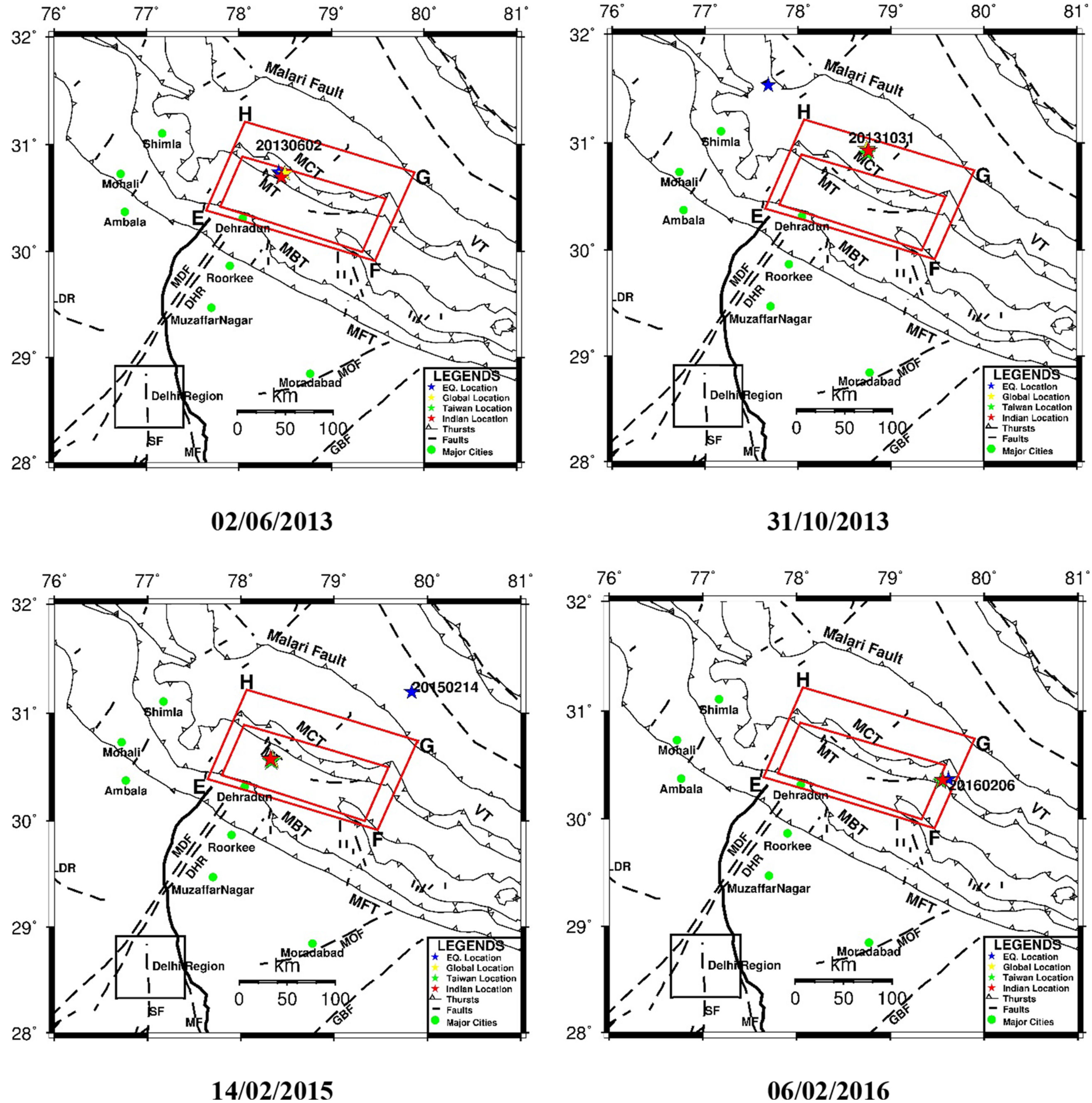

Fig. 7 Estimated location for various transformed earthquakes in India using three different velocity models

14/2/2015 earthquake

This earthquake is located toward the northeast side of instrumentation window. As that of 31/10/2013 earthquake, the system responds to this earthquake, but the location as well as depth is worst for this earthquake. The system responds 11 s after P-wave arrival and that also with triggering of 12 instruments. Using the first report, the earthquake is located toward the southwest side of instrumentation window. By the time the second report is generated, 16 s had elapsed, but no change is found in the location of the earthquake (Fig. 7). The estimated magnitude by all three models is also very absurd. M_{P_d} estimated using global model is 5.2, while using Taiwan and Indian velocity model it is reported to be $M_{P_d} = 7.7$, which is nowhere close to actual magnitude. This earthquake is located offshore in Taiwan, and no instruments were close to this earthquake, a high location and depth error was obtained. In India also, this earthquake is located in inhabitant area (where no EEW sensor is available), so a precise location is not obtained using EEW.

23/3/2015 earthquake

The earthquake of March 23, 2015 is located far but on the top of instrumentation window. Although the system responded somewhat late to this earthquake as compared to earthquakes located within instrumentation window or close to it, still a better location is found as compared to earthquakes very far away from the window. The first report is generated around 10 s after P-wave arrival using Taiwan and Global velocity model (Fig. 8a). Till this time the system with Indian velocity model did not respond. Using Taiwan and velocity model, the location of the earthquake is very far away from actual one. By the time Taiwan and Global velocity model generate third and fourth report (Fig. 8b, c), the Indian model generates second report (Fig. 8c). The location as well as depth reported by the system using Indian velocity model is very close to actual one, while using Taiwan and Global velocity model it is very far.

6/2/2016 earthquake

This earthquake is an inland earthquake in Taiwan and a bigger one in recent time. This earthquake caused destruction in Taiwan (117 casualties and 550 injured) because of the collapse of one complete residential building. When transformed to India, this earthquake is situated toward the eastern side of instrumentation window. The system responded very well to this earthquake with all three velocity models; however, the initial time of reporting is around 12.5 s. The source directivity may be the one reason for taking that much time for system to respond. If some of the instruments were installed toward the eastern side of earthquake location; the system could have responded faster with better accuracy. By the time the third and fourth reports are generated which is approximately 16.0 s after P-wave arrival (Fig. 7); a precise location is obtained, but depth is not that accurate. Looking closely at the figure, it can be found that system with Indian velocity model provides the location close to the actual earthquake as compared to others.

Synthetic records

Since the earthquakes used in present work were recorded in Taiwan having different tectonics, which may have different waveforms and may not be valid in the Himalayan region of India. In the absence of any big earthquake recorded by this network and to validate our results, we generated synthetic seismograms at all stations of the EEW network in India from the epicenter of historical Chamoli earthquake of 1999 (M_w 6.5) and Uttarkashi earthquake of 1991 (M_w 6.8). The synthetic waveforms for Chamoli and Uttarkashi earthquakes are generated at 82 points, where IIT Roorkee has installed EEW instruments. The interspacing between these instruments is generally less than 15–20 km, but at some points, this spacing is more than 20 km keeping in mind the proper logistics. Synthesis of the accelerograms of both earthquakes is carried out using modified stochastic model based on dynamic corner frequency proposed by Motazedian and Atkinson (2005). This technique has been applied successfully previously in Himalayan region (Mittal and Kumar 2015; Mittal et al. 2016b), and results are comparable. The various region-specific and general parameters are required for carrying out synthesis. The detail of these parameters is given in Table 3. The synthetic accelerograms were compared with the recorded one at few stations in terms of peak ground acceleration (PGA) and looks satisfactory. Additionally, the synthetic accelerograms were also compared in terms of PGA using attenuation relationships valid for

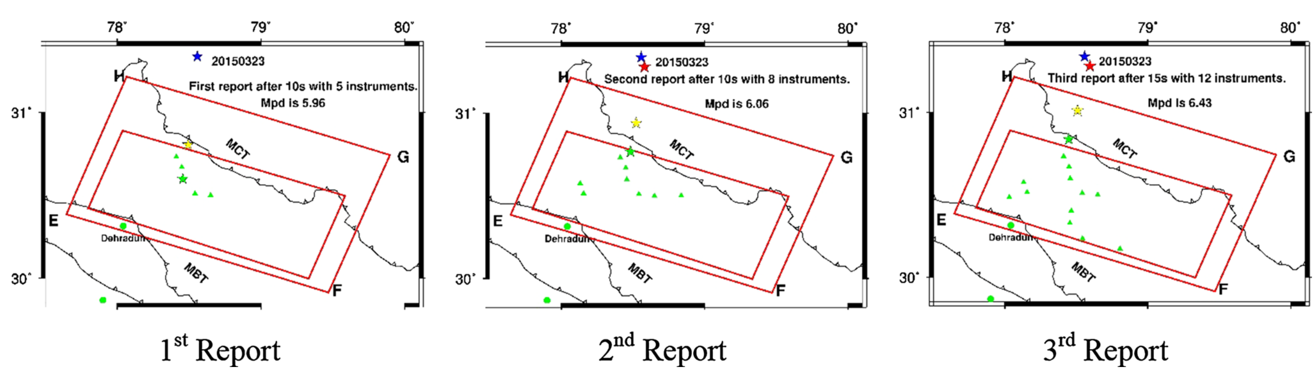

Fig. 8 Various reports generated after different time during 23/3/2015 earthquake. Blue star depicts the transformed earthquake location in Indian coordinate systems. Yellow star, green star and red star gives the location estimated in EEW system using global velocity model, Taiwan velocity model and Indian velocity model, respectively. A good location estimate is obtained using Indian velocity model compared to Global and Taiwan velocity model

Table 3 Details of various parameters used for generation of synthetic accelerograms from the epicenter of historical Chamoli (1999) and Uttarkashi (1991) earthquake

Parameter	Parameter value	
	Chamoli	Uttarkashi
Latitude, longitude	30.38°N, 79.21°E (CMT catalogue)	30.78°N, 78.77°E (USGS)
Fault orientation (strike, dip)	280°, 7° (CMT catalogue)	296°, 5° (USGS)
Fault length and width (km)	20, 12 (Wells and Coppersmith 1994)	26,18 (Wells and Coppersmith 1994)
Subfault length and width (km)	2, 2	2, 2
Depth of the hypocenter (km)	15.0 (CMT catalogue)	10.0 (USGS)
Moment magnitude (M_w)	6.5 (CMT catalogue)	6.8 (USGS)
$Q(f)$	$87f^{0.71}$ (Sharma et al. 2009)	$87f^{0.71}$ (Sharma et al. 2009)
Distance-dependent duration	0 ($R<10$ km), $0.16R$ ($10<R<70$ km), $-0.03R$ ($70<R<130$ km), $0.04R$ ($R>130$ km) (Beresnev and Atkinson 1999)	0 ($R<10$ km), $0.16R$ ($10<R<70$ km), $-0.03R$ ($70<R<130$ km), $0.04R$ ($R>130$ km) (Beresnev and Atkinson 1999)
Kappa (s)	0.04	0.04
Crustal shear-wave velocity (km/s)	3.6	3.6
Crustal density (g/cm^3)	2.8	2.8
Geometric spreading	$1/R^{1.2}(R \leq 100\,\text{km})$ $1/R^{0.5}(R > 100\,\text{km})$ Singh et al. (1999) with little change	$1/R^{1.2}(R \leq 100\,\text{km})$ $1/R^{0.5}(R > 100\,\text{km})$ Singh et al. (1999) with little change
Stress parameter (bars)	60 (Singh et al. 2002)	55 (Kumar et al. 2012a)
Pulsing percentage	50%	50%
Windowing function	Saragoni–Hart	Saragoni–Hart
Rupture velocity/shear-wave velocity	0.8	0.8
Crustal amplification	Western North America generic rock site (Boore and Joyner 1997)	Western North America generic rock site (Boore and Joyner 1997)

Himalayan region (Sharma 1998), and results are found in agreement.

The synthetic waveforms at all 82 stations from both Chamoli and Uttarkashi earthquakes are combined into two separate files called Tank files. These files are passed through the Earthworm software in a similar manner, as these would have streamed during real-time event. The algorithm is then tested, and the parameter values can be optimized. Earthworm module Pick_EEW automatically detects the P-wave arrival based on STA/LTA algorithms proposed by Allen et al. (2009) and Allen (1978), and the peak values of displacement (P_d), velocity (P_v) and acceleration (P_a) are estimated from 3 s time window after the P-wave arrival as mentioned earlier for the Taiwan events. The sensitivity using Allen (1978) may be low as we are interested in higher magnitude events. All the calculations related to Chamoli and Uttarkashi earthquake in Earthworm software are made by replacing Taiwan velocity model with Indian velocity model. All the threshold values in algorithm are based on Wu and Kanamori (2008), as they found threshold values of different parameters using strong motion data from 11 events in Taiwan, 26 events in Southern California and 17 events from Japan. According to them if P_d is 0.5 cm, then the corresponding PGV will be 20 cm/s and the earthquake will be damaging.

Chamoli earthquake (1999)

Chamoli earthquake is one of the historical earthquakes in CSG Himalayas that caused widespread damage in the region. Around 100 people died and thousands injured because of this earthquake. This earthquake is well located within the instrumentation window, and the system responds efficiently to this earthquake. The analysis for synthetic records is carried out using Indian velocity model only as these were generated using parameters valid for the region. The system generates first report in 5.5 s with triggering of 15 instruments (Fig. 9). Significant error is reported in location as well as magnitude. Fourth report is generated in 8.5 s with triggering of 25 instruments (Fig. 9). The location as well as depth is close to one reported by the Harvard CMT catalogue. The calculated M_{P_d} is 6.9, which is slightly higher than the actual one. By the time, eighth report is generated with 42 instruments, the estimated magnitude, location as well as depth becomes stable (Fig. 9). The final estimated M_{P_d} is 6.83, while depth is 22 km, which is more than reported by Harvard CMT catalogue. This slight difference in magnitude may be attributed to near-field term, which may lead to the higher P_d values. Also, since these records are synthetic and not actual, a lot of factors like stress drop may affect different parameters estimation. However, there

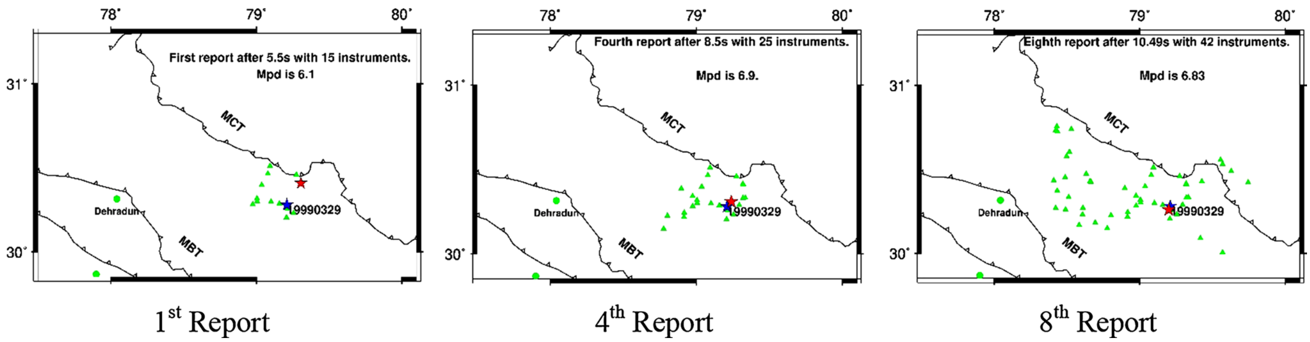

Fig. 9 Various reports generated for 1999 Chamoli earthquake using synthetic records. A good location as well as magnitude estimation is found using Indian velocity model. The blue star represents the earthquake location of 1999 Chamoli earthquake, while red star gives the estimated location using synthetic records in EEW system

is discrepancy between different agencies regarding the magnitude, depth and location of this earthquake. Indian Meteorological Department (IMD, the official agency for reporting earthquakes in India) reported its magnitude to be 6.8 having a depth of 21 km. In total, 16 reports are generated for this earthquake.

Uttarkashi earthquake (1991)

Uttarkashi earthquake of 1991 is another big earthquake that occurred in this region and falls outside instrumentation window. No station is found close to the epicenter of this earthquake. So the first report is generated 12.3 s later with triggering of 16 instruments (Fig. 10). The resulting location, magnitude and depth are far away from actual one. Total 10 reports are generated for this earthquake. The sixth report is generated 17.73 s later with triggering of 38 instruments (Fig. 10). The reported M_{P_d} is found to be 6.20, while the depth is 20.7 km. The location is also slightly away from the actual location. In all following reports, no change is found in location, magnitude and depth. This difference may be attributed to insufficient station coverage as well as synthetic record.

An EEW system is considered to reliable that provides maximum lead time as well as precise location and magnitude (having minimum error in magnitude estimation as well as location). When enough station coverage is there, too many variations are not found in the location using all three velocity models. By the time the fourth report is generated which takes approximately 10–15 s, a reliable location, as well as magnitude, is obtained. For earthquakes of March 27, 2013; June 2, 2013 and February 6, 2016 located between Main Boundary Thrust (MBT) and Main Central Thrust (MCT), which may be the location of future higher magnitude in the Himalayas, a high lead time is obtained for the plainer region using this EEW instrumentation. However, for the earthquake of February 6, 2016, the system will be able to respond in a fast and efficient way if some of the instruments are also installed toward eastern side. For the earthquake of October 31, 2013, instrumentation should be extended toward the western side. For the earthquake of February 14, 2015, which lies in an inhabitant area, we

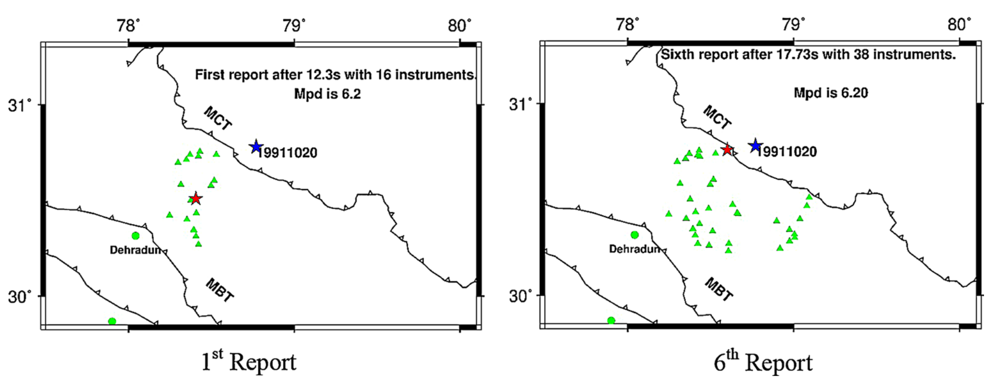

Fig. 10 Various reports generated for 1991 Uttarkashi earthquake using synthetic records. The blue star represents the earthquake location of 1991 Uttarkashi earthquake, while red star gives the estimated location using synthetic records in EEW system. The difference in location, magnitude and depth is reported which may be due to synthetic records and insufficient station coverage as no station is situated close to epicenter location

understand that instrumentation would be difficult. For detecting earthquakes like March 23, 2015 in a better way, it will be good to spread instrumentation toward the north. Using synthetic records of Chamoli and Uttarkashi earthquake in this study, same kind of results are obtained. For Chamoli earthquake, a reliable location as well as magnitude estimation is reported. However, for Uttarkashi earthquake, significant difference in location as well as magnitude is found which may be due to the insufficient coverage as no instrument lies toward north of epicenter and due to the synthetic nature of records. From here, it can be inferred that this instrumentation may provide good lead time from earthquake situated between MBT and MCT in instrumentation window. We are using P-Alert data from Taiwan, and this instrumentation has not recorded any earthquake having magnitude $M_w > 7$ since its installation. All the earthquakes that we have used have the magnitude (M_w) between 5.5 to 7.0, so P_d approach using three seconds may be efficient to estimate magnitude in a reliable way as the magnitude is close to actual one (Table 2). For earthquakes having magnitude $M_w > 7.0$ like Tohoku, Japan earthquake ($M_w = 9.1$), this approach using 3 s may be insufficient as the fault may be still rupturing and magnitude may be underestimated. In recent time, Chen et al. (2017) used different time windows (1–10 s) for calculating the magnitude for such big earthquakes and concluded that using few second window initially from recorded waveforms and then updating it with increasing time window may provide useful results. Nevertheless, this kind of approach using high time windows may reduce the early warning time. From regional EEW point of view, this instrumentation is built to provide enough warning time for cities in Himalayan foothills and plainer regions like Dehradun, Haridwar, Roorkee, Ambala, Mohali, Chandigarh, Muzaffarnagar, Meerut, Delhi NCR and so on. Figure 11 depicts the lead time warning for different cities from the earthquake of June 2, 2013 situated between MBT and MCT. For Delhi NCR region, which is approximately 270 km away from this earthquake situated between MBT and MCT, 65–70 s of lead time may be a reliable approximation. Dehradun is the closest city so lead time may be least as compared to other cities mentioned above. Bhardwaj et al. (2016) used data from Japan and India to calculate various EEW parameters like maximum predominant period (τ_p^{max}), τ_c, P_d, cumulative absolute velocity (CAV), bracketed cumulative absolute velocity (BCAV), windowed bracketed cumulative average velocity (BCAV-W) and root sum of squares cumulative velocity (RSSCV). They used the dataset from

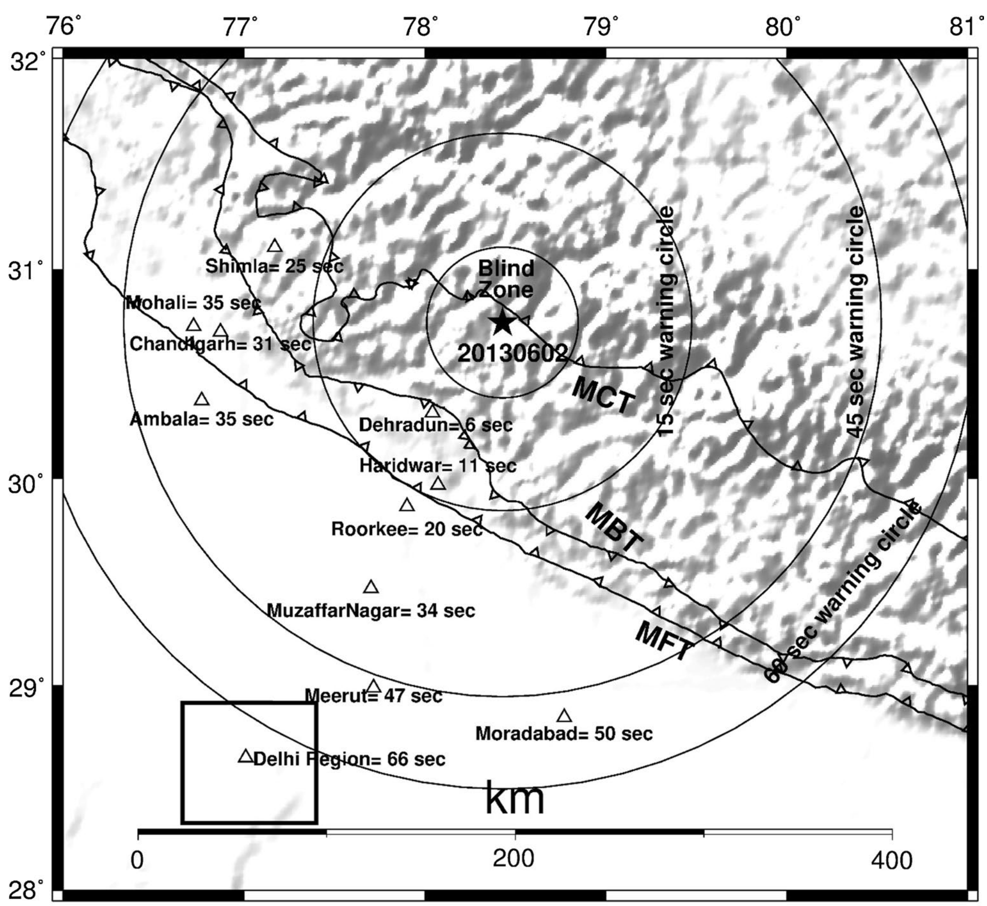

Fig. 11 The lead time for various cities in foothills of Himalayas and plainer regions from earthquake of June 2, 2013 located between MBT and MCT. Blind zone where no regional warning is possible is also shown. Maximum lead time is obtained for Delhi region, which is 270 km away from earthquake source, while minimum lead time is for Dehradun city, which is around 60 km away

Japan having magnitude $5 \leq M \leq 7$ with epicentral distance ≤ 60 km. From India, they choose dataset having $3.3 \leq M \leq 6.6$ with epicentral distance ≤ 60 km. This dataset in India is recorded by National strong instrumentation network across the Himalayas having interstation spacing around 40 km (Kumar et al. 2012b; Mittal et al. 2006, 2012). In light of their findings, they found that P_d is a descent indicator of EEW; however, the combination of two or three EEW parameters might always be a better option. The dataset recorded by this instrumentation in India provides an excellent opportunity to carry out some useful works (Mittal et al. 2013b, 2016a, c). Seismic hazard for Delhi region (the region of interest for EEW) is estimated previously in terms of site effects and spectral acceleration using data from this network (Mittal et al. 2013a, c, 2015). Bhardwaj et al. (2016) performed analysis considering few earthquakes from India having sparse records before deployment of EEW network in India. However, for EEW in operation, a closely spaced instrumentation is much needed.

Conclusions

The seismicity in India has been well reflected in its seismic zonation map of Indian Government where more than 60% of the area is under high seismic risk. It has got almost similar seismic hazard as those countries where the EEW systems are well established and have been used successfully for disaster mitigation and management. The complicated seismicity in the Himalayas affects whole northern India and northeast India. On the other hand, instrumenting the entire Himalayan Belt region is not easy because of its length (2500 km). IIT Roorkee initialized EEW in the northern Himalayas by installing about 100 seismic stations in a specific belt in CSG. In this paper, we have focused more on the applicability of EEW using recorded data from Taiwan, as no recorded ground data from larger magnitude earthquake are available in India for checking the functionality of EEW. Recorded ground motion data from Taiwan provide an excellent opportunity to test the feasibility of EEW in northern India. The system performs very well in terms of earthquake detection, P-wave picking, earthquake magnitude and location (using previously estimated regressions) using P_d algorithm. For the earthquakes situated between MBT and MCT, and close to instrumentation window, a good estimate of location as well as magnitude is found. Since the earthquakes used in present study are recorded in Taiwan having different tectonics, so the recorded waveforms may not be same as that of India. In order to support our results, we generated synthetic seismograms from the epicenter of historical Chamoli (1999) and Uttarkashi (1991) earthquake at EEW stations in India. We checked the functionality of EEW using these synthetic seismograms. The Chamoli earthquakes are located within the instrumentation window; a good approximation of earthquake location and magnitude is obtained by passing these generated waveforms. The Uttarkashi earthquake is located out of the instrumentation window, no station is found toward north of the epicenter, and the results are found to differ from actual one. It is observed when the number of stations is more and closely spaced, as that of Taiwan, a good approximation of earthquake location as well as magnitude is found. On the other hand, when the number of instruments is less and earthquake location falls away from the instrumentation window, a marginal error is observed in earthquake location. From here, it can be concluded that for EEW to operate satisfactorily in India and to get EEW at least from earthquakes originating in seismic gaps in the Himalayas, the number of instruments should be increased drastically.

Data and resources

Earthquake data used in this study are obtained from P-Alert instrumentation network managed by National Taiwan University (NTU) of Taiwan. The GMT software from Wessel and Smith (1998) was used in plotting part of the figures and is gratefully acknowledged.

Acknowledgments The authors are profusely thankful to Ministry of Science and Technology (MOST) of Taiwan for funding the project (106-2116-M-002-019-MY3), under which this study was carried out. Cédric Legendre, Academia Sinica and Professor Ting-Li Lin, NCKU are greatly acknowledged for careful checking of manuscript. The authors are really thankful to two anonymous reviewers and CO-EDITOR-IN-CHIEF Ramon Zuñiga, for their constructive comments, which helped in improving the manuscript.

Compliance with ethical standards

Conflict of interest On behalf of all authors, the corresponding author states that there is no conflict of interest.

References

Alcik H, Ozel O, Apaydin N, Erdik M (2009) A study on warning algorithms for Istanbul earthquake early warning system. Geophys Res Lett 36:L00B05. https://doi.org/10.1029/2008gl036659

Allen R (1978) Automatic earthquake recognition and timing from single traces. Bull Seismol Soc Am 68:1521–1532

Allen RM, Kanamori H (2003) The potential for earthquake early warning in southern California. Science 300:786–789

Allen RM, Brown H, Hellweg M, Khainovski O, Lombard P, Neuhauser D (2009) Real-time earthquake detection and hazard assessment by ElarmS across California. Geophys Res Lett 36:L00B08. https://doi.org/10.1029/2008gl036766

Beresnev IA, Atkinson GM (1999) Generic finite-fault model for ground motion prediction in eastern north America. Bull Seismol Soc Am 89(3):608–625

Bhardwaj R, Sharma ML, Kumar A (2016) Multi-parameter algorithm for earthquake early warning. Geomat Nat Hazards Risk 7(4):1242–1264. https://doi.org/10.1080/19475705.2015.1069409

Bilham R (1995) Location and magnitude of the Nepal earthquake and its relation to the rupture zones of the contiguous great Himalayan earthquakes. Curr Sci 69:101–128

Boore DM, Joyner WB (1997) Site amplifications for generic rock sites. Bull Seismol Soc Am 87:327–341

Böse M, Ionescu C, Wenzel F (2007) Earthquake early warning for Bucharest, Romania: novel and revisited scaling relations. Geophys Res Lett 34:L07302. https://doi.org/10.1029/2007gl029396

Böse M, Hauksson E, Solanki K, Kanamori H, Heaton TH (2009) Real-time testing of the on-site warning algorithm in southern California and its performance during the July 29, 2008 M_w 5.4 Chino Hills earthquake. Geophys Res Lett 36:L00B03. https://doi.org/10.1029/2008gl036366

Brown HM, Allen RM, Hellweg M, Khainovski O, Neuhauser D, Souf A (2011) Development of the ElarmS methodology for earthquake early warning: realtime application in California and offline testing in Japan. Soil Dyn Earthq Eng 31(2):188–200

Carranza M, Buforn E, Colombelli S, Zollo A (2013) Earthquake early warning for southern Iberia: a P wave threshold-based approach. Geophys Res Lett 40(17):4588–4593. https://doi.org/10.1002/grl.50903

Chen DY, Hsiao NC, Wu YM (2015) The Earthworm-based earthquake alarm reporting system in Taiwan. Bull Seismol Soc Am 105:568–579

Chen DY, Wu YM, Chin TL (2017) An empirical evolutionary magnitude estimation for early warning of earthquakes. J Asian Earth Sci 135:190–197

Cua G, Heaton T (2007) The Virtual Seismologist (VS) method: a Bayesian approach to earthquake early warning. In: Gasparini P, Manfredi G, Zschau J (eds) Earthquake early warning systems. Springer, Heidelberg, pp 97–132

Erdik M, Fahjan Y, Ozel O, Alcik H, Mert A, Gul M (2003) Istanbul earthquake rapid response and the early warning system. Bull Earthq Eng 1:157–163

Espinosa-Aranda JM, Jimenez A, Ibarrola G, Alcantar F, Aguilar A (1995) Mexico City seismic alert system. Seismol Res Lett 66:42–53

Espinosa-Aranda JM, Cuellar A, Garcia A, Ibarrola G, Islas R, Maldonado S, Rodriguez FH (2009) Evolution of the Mexican Seismic Alert System (SASMEX). Seismol Res Lett 80(5):694–706. https://doi.org/10.1785/gssrl.80.5.694

Gupta S (2000) Development in strong motion instrumentation of nuclear power plant sites. In: Symposium on Seismology, earthquake hazard assessment and earth's interior related topics, Asian Seismological Commission (ASC), Tehran, Iran

Hoshiba M, Kamigaichi O, Saito M, Tsukada S, Hamada N (2008) Earthquake early warning starts nationwide in Japan. EOS Trans AGU 89(8):73–74

Hsiao NC, Wu YM, Shin TC, Zhao L, Teng TL (2009) Development of earthquake early warning system in Taiwan. Geophys Res Lett 36:L00B02. https://doi.org/10.1029/2008gl036596

Ionescu C, Böse M, Wenzel F, Marmureanu A, Grigore A, Marmureanu G (2007) Early warning system for deep Vrancea (Romania) earthquakes. In: Gasparini P, Manfredi G, Zschau J (eds) Earthquake early warning systems. Springer, Heidelberg, pp 343–349

Johnson CE, Bittenbinder A, Bogaert B, Dietz L, Kohler W (1995) Earthworm: a flexible approach to seismic network processing. IRIS Newsl 14:4

Kamigaichi O, Saito M, Doi K, Matsumori T, Tsukada S, Takeda K, Shimoyama T, Nakamura K, Kiyomoto M, Watanabe Y (2009) Earthquake early warning in Japan: warning the general public and future prospects. Seismol Res Lett 80(5):717–726

Kanamori H (2005) Real-time seismology and earthquake damage mitigation. Annu Rev Earth Planet Sci 33:195–214. https://doi.org/10.1146/annurev.earth.33.092203.122626

Kennett BLN, Engdahl ER (1991) Travel times for global earthquake location and phase association. Geophys J Int 105:429–465

Khattri KN (1999) An evaluation of earthquakes hazard and risk in northern India. Himal Geol 20:1–46

Kumar N, Sharma J, Arora BR, Mukhopadhyay S (2009) Seismotectonic model of the Kangra–Chamba sector of Northwest Himalaya: constraints from joint hypocenter determination and focal mechanism. Bull Seismol Soc Am 99(1):95–109

Kumar A, Kumar A, Kumar A, Gupta SC, Jindal AK, Mittal H (2012a) Source parameters of Uttarkashi earthquake of 21st Sept. In: 15th world conference on earthquake engineering, Lisbon, Portugal, 24–28 Sept 2012, pp 4060–4067. ISBN: 978-1-63439-651-6

Kumar A, Mittal H, Sachdeva R, Kumar A (2012b) Indian strong motion instrumentation network. Seismol Res Lett 83(1):59–66

Kumar A, Mittal H, Chamoli BP, Gairola A, Jakka RS, Srivastava A (2014) Earthquake early warning system for northern India. In: 15th symposium on earthquake engineering, Indian Institute of Technology, Roorkee, 11–13 Dec 2014, pp 231–238. Elite Publishing, New Delhi

Legendre CP, Zhao L, Chen QF (2015a) Upper-mantle shear-wave structure under East and Southeast Asia from Automated Multimode Inversion of waveforms. Geophys J Int 203(1):707–719

Legendre CP, Deschamps F, Zhao L, Chen QF (2015b) Rayleigh-wave dispersion reveals crust-mantle decoupling beneath eastern Tibet. Sci Rep 5:16644

Legendre CP, Tseng TL, Mittal H, Hsu CH, Karakhanyan A, Huang BS (2017) Complex wave propagation revealed by peak ground velocity maps in the caucasus area. Seismol Res Lett 88(3):812–821

Mittal H, Kumar A (2015) Stochastic finite-fault modeling of M_w 5.4 earthquake along Uttarakhand-Nepal border. Nat Hazards 75(2):1145–1166

Mittal H, Gupta S, Srivastava A, Dubey RN, Kumar A (2006) National strong motion instrumentation project: an overview. In: 13th symposium on earthquake engineering, Indian Institute of Technology, Roorkee, 18–20 Dec 2006, pp 107–115. Elite Publishing, New Delhi

Mittal H, Kumar A, Ramhmachhuani R (2012) Indian national strong motion instrumentation network and site characterization of its stations. Int J Geosci 3(6):1151–1167

Mittal H, Kamal, Kumar A, Singh SK (2013a) Estimation of site effects in Delhi using standard spectral ratio. Soil Dyn Earthq Eng 50:53–61

Mittal H, Kumar A, Kamal (2013b) Ground motion estimation in Delhi from postulated regional and local earthquakes. J Seismol 17(2):593–605. https://doi.org/10.1007/s10950-012-9340-5

Mittal H, Kumar A, Kumar A (2013c) Site effects estimation in Delhi from the Indian strong motion instrumentation network. Seismol Res Lett 84(1):33–41

Mittal H, Kumar A, Kumar A, Kumar R (2015) Analysis of ground motion in Delhi from earthquakes recorded by strong motion network. Arab J Geosci 8(4):2005–2017

Mittal H, Kumar A, Wu YM, Kumar A (2016a) Source study of M_w 5.4 April 4, 2011 India–Nepal border earthquake and scenario events in the Kumaon–Garhwal Region. Arab J Geosci 9(5):348

Mittal H, Wu YM, Chen DY, Chao WA (2016b) Stochastic finite modelling of ground motion for March 5th 2012 M_w 4.6 earthquake and scenario greater magnitude earthquake in the proximity of Delhi. Nat Hazards 82(2):1123–1146. https://doi.org/10.1007/s11069-016-2236-x

Mittal H, Wu YM, Kumar A, Kumar A, Sharma B (2016c) Evaluating the effects of ground motion parameters on response spectra in Uttarakhand Himalayas, India. Arab J Geosci 9(18):712

Motazedian D, Atkinson GM (2005) Stochastic finite-fault modeling based on dynamic corner frequency. Bull Seismol Soc Am 95:995–1010

Nakamura Y (1988) On the urgent earthquake detection and alarm system (UrEDAS). In: Proceedings of the 9th world conference on earthquake engineering, Tokyo–Kyoto, Japan, 2–9 Aug 1988, pp 673–678

Pazos A, Romeu N, Lozano L, Colom Y, López Mesa M, Goula X, Jara JA, Cantavella JV (2015) A regional approach for earthquake early warning in southwest Iberia: a feasibility study. Bull Seismol Soc Am 105(2A):560–567. https://doi.org/10.1785/0120140101

Petit NR, Puyané YC, Salvador JAJ, Suriñach XG, Vidal TS (2016) Development of an earthquake early warning system based on earthworm: application to Southwest Iberia. Bull Seismol Soc Am 106(1):1–12

Satriano C, Wu YM, Zollo A, Kanamori H (2011) Earthquake early warning: concepts, methods and physical grounds. Soil Dyn Earthq Eng 31:106–118. https://doi.org/10.1016/j.soildyn.2010.07.007

Seeber L, Armbruster JG (1981) Great detachment earthquakes along the Himalayan arc and long-term forecasting. Earthq Predict Int Rev 4:259–277

Sharma ML (1998) Attenuation relationship for estimation of peak ground horizontal acceleration using data from strong-motion arrays in India. Bull Seismol Soc Am 88(4):1063–1069

Sharma ML (2003) Seismic hazard in northern India region. Seismol Res Lett 74(2):140–146

Sharma ML, Lindolhm C (2012) Earthquake hazard assessment for Dehradun, Uttarakhand, India, including a characteristic earthquake recurrence model for the Himalaya Frontal Fault (HFF). Pure Appl Geophys 169:1601–1617

Sharma B, Teotia SS, Kumar D, Raju PS (2009) Attenuation of P-and S-waves in the Chamoli Region, Himalaya, India. Pure Appl Geophys 166(12):1949

Shieh JT, Wu YM, Zhao L, Chao WA, Wu CF (2011) An examination of τ_c-Pd earthquake early warning method using a strong motion building array. Soil Dyn Earthq Eng 31(2):240–246

Singh SK, Ordaz M, Dattatrayam RS, Gupta HK (1999) A spectral analysis of the May 21, 1997, Jabalpur, India earthquake ($M_w = 5.8$) and estimation of ground motion from future earthquakes in the Indian shield region. Bull Seismol Soc Am 89:1620–1630

Singh SK, Mohanty WK, Bansal BK, Roonwal GS (2002) Ground motion in Delhi from future large/great earthquakes in the central seismic gap of the Himalayan arc. Bull Seismol Soc Am 92:555–569

Vincenty T (1975) Direct and inverse solutions of geodesics on the ellipsoid with application of nested equations. Surv Rev 23(176):88–93. http://www.ngs.noaa.gov/PUBS_LIB/inverse.pdf

Wells DL, Coppersmith KJ (1994) New empirical relationships among magnitude, rupture length, rupture width, rupture area, and surface displacement. Bull Seismol Soc Am 84:974–1002

Wenzel F, Onescu M, Baur M, Fiedrich F (1999) An early warning system for Bucharest. Seismol Res Lett 70:161–169

Wessel P, Smith WH (1998) New, improved version of generic mapping tools released. Eos Trans Am Geophys Union 79(47):579

Wu YM (2015) Progress on development of an earthquake early warning system using low cost sensors. Pure Appl Geophys 172:2343–2351. https://doi.org/10.1007/s00024-014-0933-5

Wu YM, Kanamori H (2005a) Experiment on an onsite early warning method for the Taiwan early warning system. Bull Seismol Soc Am 95:347–353

Wu YM, Kanamori H (2005b) Rapid assessment of damage potential of earthquakes in Taiwan from the beginning of P waves. Bull Seismol Soc Am 95:1181–1185

Wu YM, Kanamori H (2008) Development of an earthquake early warning system using real-time strong motion signals. Sensors 8:1–9

Wu YM, Zhao L (2006) Magnitude estimation using the first three seconds P-wave amplitude in earthquake early warning. Geophys Res Lett 33:L16312. https://doi.org/10.1029/2006gl026871

Wu YM, Yen HY, Zhao L, Huang BS, Liang WT (2006) Magnitude determination using initial P waves: a single station approach. Geophys Res Lett 33:L05306. https://doi.org/10.1029/2005gl025395

Wu YM, Kanamori H, Allen R, Hauksson E (2007) Determination of earthquake early warning parameters, τ_c and P_d, for southern California. Geophys J Int 170:711–717. https://doi.org/10.1111/j.1365-246x.2007.03430.x

Wu YM, Lin TL, Chao WA, Huang HH, Hsiao NC, Chang CH (2011) Faster short-distance earthquake early warning using continued monitoring of filtered vertical displacement—a case study for the 2010 Jiasian earthquake, Taiwan. Bull Seismol Soc Am 101:701–709. https://doi.org/10.1785/0120100153

Wu YM, Chen DY, Lin TL, Hsieh CY, Chin TL, Chang WY, Li WS, Ker SH (2013) A high density seismic network for earthquake early warning in Taiwan based on low cost sensors. Seismol Res Lett 84:1048–1054. https://doi.org/10.1785/0220130085

Wu YM, Liang WT, Mittal H, Chao WA, Lin CH, Huang BS, Lin CM (2016) Performance of a low-cost earthquake early warning system (P-Alert) during the 2016 M_L 6.4 Meinong (Taiwan) earthquake. Seismol Res Lett 87(5):1050–1059. https://doi.org/10.1785/0220160058

Wu YM, Mittal H, Huang TC, Yang BM, Jan JC, Chen SK (2018) Performance of a low-cost earthquake early warning system (P-Alert) and shake map production during the 2018 M_w 6.4 Hualien (Taiwan) earthquake. Seismol Res Lett. https://doi.org/10.1785/0220180170

Wyss M, Gupta S, Rosset P (2017) Casualty estimates in two up-dip complementary Himalayan earthquakes. Seismol Res Lett 88:1508–1515

Yamada M, Heaton T (2008) Real-time estimation of fault rupture extent using envelopes of acceleration. Bull Seismol Soc Am 98:607–619

Yamada M, Mori J (2009) Using τ_c to estimate magnitude for earthquake early warning and effects of near-field terms. J Geophys Res Solid Earth. https://doi.org/10.1029/2008JB006080

Zollo A, Lancieri M, Nielsen S (2006) Earthquake magnitude estimation from peak amplitudes of very early seismic signals on strong motion records. Geophys Res Lett 33:L23312. https://doi.org/10.1029/2006gl027795

Zollo A, Iannaccone G, Lancieri M, Convertito V, Emolo A, Festa G, Gallovic F, Vassallo M, Martino C, Satriano C et al (2009) Earthquake early warning system in southern Italy: methodologies and performance evaluation. Geophys Res Lett 36:L00B07. https://doi.org/10.1029/2008gl036689